Tip-enhanced Raman spectroscopy of graphite irradiated by focused ion beam

Tsu-Shin Chan,[1,2] Mykhaylo M. Dvoynenko,[1,3] Chih-Yi Liu,[1,4] Juen-Kai Wang,[1,5] and Yuh-Lin Wang[1,6]

[1]*Institute of Atomic and Molecular Sciences, Academia Sinica, Taipei 106, Taiwan*
[2]*Department of Chemistry, National Taiwan University, Taipei 106, Taiwan*
[3]*Institute of Semiconductor Physics, National Academy of Sciences of Ukraine, Kyiv 03028, Ukraine*
[4]*Institute of Innovations and Advanced Studies (IIAS), National Cheng Kung University, Tainan 701, Taiwan*
[5]*Center for Condensed Matter Sciences, National Taiwan University, Taipei 106, Taiwan (jkwang@ntu.edu.tw)*
[6]*Department of Physics, National Taiwan University, Taipei 106, Taiwan (ylwang@pub.iams.sinica.edu.tw)*

Received March 26, 2009; revised June 19, 2009; accepted June 21, 2009;
posted June 25, 2009 (Doc. ID 110218); published July 17, 2009

Tip-enhanced Raman spectroscopy with a spatial resolution of 25 nm is conducted on a sample of graphite that has been exposed to a 50 keV focused Ga ion beam with a diameter of 20 nm. The G mode located at 1579 cm^{-1} does not exhibit a measurable tip enhancement, while the D mode at 1364 cm^{-1} is significantly enhanced. A method is proposed to calculate the enhancement factor of anisotropic materials due to the electromagnetic field using the measured signal enhancement induced by the tip. © 2009 Optical Society of America

OCIS codes: 240.6695, 180.5655, 180.4243, 180.5810, 300.6330, 290.5860.

Recent interest in graphitic systems [1–3] was revived by the discovery of strictly two-dimensional free-standing graphene [1], which has an unusual scattering-free electron transport behavior [2] that may lead to device applications [3]. It is thus of great importance to investigate graphitic structural defects that are the main source of resistance to electron conduction. Because of its high structure-sensitive analytic ability, Raman spectroscopy has become one of the most important characterization tools to investigate structural variation in graphitic systems [4]. Different graphitic structural defects have been revealed in Raman spectra [5–7]. In particular, Raman spectroscopy was used to study graphitic edge structures [5]. Phonon correlation length of ion-irradiated graphite was obtained from Raman spectra [6] and the planar graphitic domain was extracted indirectly from Raman data [7]. However, questions still remain about this indirect approach because the actual size of defects or domains may be much smaller than the excitation wavelength. The recent development of tip-enhanced Raman spectroscopy (TERS) [8,9] allows for an improved spatial resolution of about 10 nm [10] and, simultaneously, considerable enhancement in the Raman scattering strength. Therefore TERS could help to shed light on the issues that are not resolvable in far-field experiments [11]. Here, we report a TERS study of nanoscale defects on graphite induced by foused-ion beam (FIB) irradiation and propose a method to estimate the electromagnetic enhancement factor for anisotropic materials.

A highly oriented pyrolytic graphite (HOPG) sample was used for this study. After pealing off surface graphene layers, it was then bombarded by a Ga FIB to produce vertical lines with a width of 150 nm and a spacing of 2 μm. The size of the pattern was 20 $\mu m \times 20$ μm. The focused beam size was 20 nm, and the ion dosage was 10^{13} ion/cm^2. Figure 1 shows the atomic force microscopy (AFM) image of the bombarded sample. In TERS measurements, a mixed-gas (Ar and Kr) ion laser beam with a wavelength of 514.5 nm served as the excitation light source. It was delivered through a single-mode fiber to an AFM on a vibration-isolated table. A laser line filter blocked the residual plasma lines in the beam, and a half-wave plate and two polarizers varied the laser polarization and power. After being reflected from a sharp-edge Raman filter, the laser beam was then focused by an aspheric lens (NA=0.5) on the sample surface in *p*-polarization configuration at an incidence angle of 55° to form a spot size of ~2.5 μm. The AFM tip was then guided to the center of the laser-illuminated region of the sample. The laser power was carefully adjusted to minimize the induced heating and damage to the tip while maintaining a good Raman signal. The resultant laser intensity at focus was $\sim 2 \times 10^8$ W/m^2. The light scattered backward was collected through the same aspheric lens, sent through

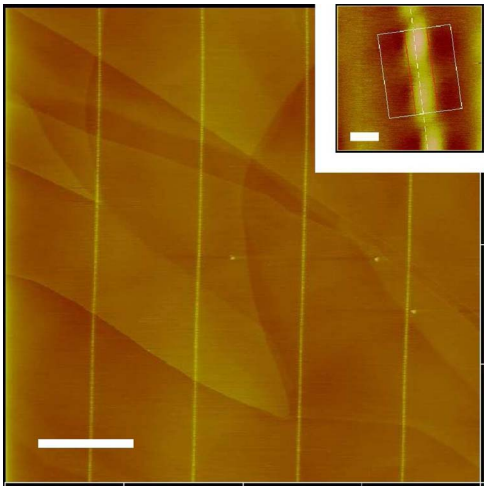

Fig. 1. (Color online) AFM images of ion-irradiated graphite sample. The scale bar is 2 μm. The inset shows the magnified view of the irradiated grid line. The scale bar in the inset is 100 nm.

0146-9592/09/152246-3/$15.00

the sharp-edge Raman filter, and then a confocal setup to a 640 mm monochromator. The dispersed spectra were detected by a liquid-nitrogen-cooled CCD with an integration time of ~5 min. The instrument spectral resolution for the slit width of 100 μm was calibrated to be 5.2 cm^{-1}. To image the tip apex, a pellicle beam splitter was used to pass fiber-coupled white light collinearly with the laser beam through the aspheric lens to the same sample region. Before being installed in the AFM, the silicon tip was cleaned with argon bombardment in a vacuum chamber (5×10^7 torr), followed by thermal evaporation of a 30–50 nm thick layer of Ag. The typical diameter of the tip apex was ~50 nm, as examined by a scanning electron microscope. During the TERS measurements, the AFM was operating in contact mode.

Figure 2 shows the Raman spectra recorded as the tip approaches the FIB-irradiated and the pristine regions of the sample. With tip withdrawn, two peaks at 1579 and 1364 cm^{-1} emerge in the spectrum, corresponding to the G and D modes, respectively. The G mode represents the optical mode of graphene at the center of the Brillouin zone, while the D mode originates from phonons at its nonzero wave vector and can be explained by defect-induced double-resonant Raman scattering [12]. The intensity of the G mode does not depend on the position of the tip. In contrast, the intensity of the D mode in the FIB-irradiated region clearly shows an increase of 4–5 times compared with that in the pristine region.

Figure 3 shows the intensity (I_D) of the D mode measured across a FIB-irradiated grid line. The profile of I_D, which can be compared with the AFM topographic profile, has a FWHM of 146 nm, reflecting the size of the disorder region caused by FIB irradiation of the sample. Based on the measurement, we deduce the lateral resolution of the TERS measurement to be ~25 nm.

An interesting question concerning the TERS measurement is: What is the enhancement factor of the D mode in the FIB-irradiated region on the sample? To answer the question, two facts need to be considered in advance. First, the field component normal to the sample surface (therefore parallel to the tip axis) $E_\perp$

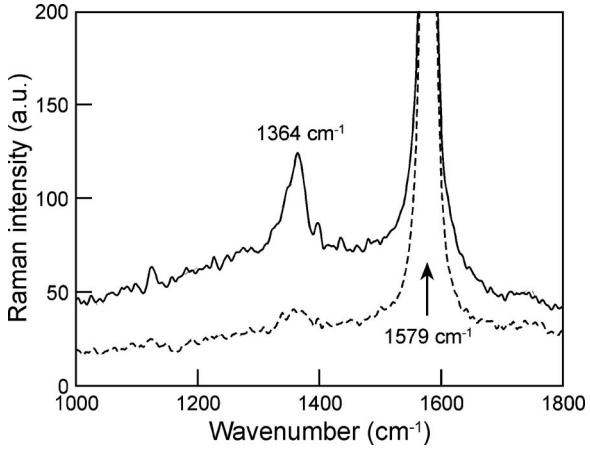

Fig. 2. Tip-enhanced Raman spectra of the sample with the engaged tip to the center of the defect line (solid curve) and out of the defect line (dashed curve).

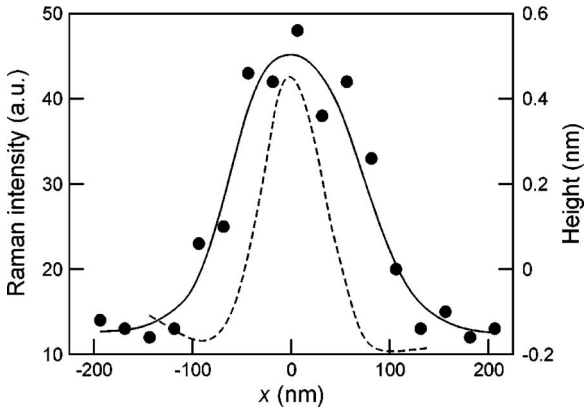

Fig. 3. Raman intensity (filled circles) and height (dashed curve) versus lateral position of the tip apex x. The solid curve is to guide the eye.

is enhanced, while that parallel to the surface $E_\parallel$ is much less enhanced [13]. Second, since the pristine graphite is a highly anisotropic system, its absorption [14] and resonant Raman scattering [15] are not sensitive to $E_\perp$, as the π electrons are symmetric with respect to the graphitic plane, forbidding electronic transition for $E_\perp$. The Raman intensity of the G mode I_G is caused by the scattering in perfect graphite and therefore depends only on $E_\parallel$. In contrast, the intensity of the defect-sensitive D mode is in general determined by both $E_\perp$ and $E_\parallel$, although in different ways. Indeed, scanning tunneling microscopy studies of ion-irradiated graphite samples showed lateral inhomogeneities of ~2 nm [16], indicating that the local orientation of graphite layers near such defects is not completely parallel to the undamaged graphite layer, causing the absorption and Raman scattering near the ion-irradiated region to be sensitive to all the field components. According to a separated far-field Raman measurement on a HOPG sample under uniform ion dosage (not shown here), the ratio between the intensity of the D mode for p polarization I_D^p and that of the G mode I_G^p is ~7–10% higher than the corresponding ratio for s polarization. As a result, the I_D of the ion-irradiated region is sensitive to $E_\perp$, too.

On the basis of the two facts above, the far-field Raman intensities of the G mode for s- and p-polarized light are given by

$$I_G^s \propto \sigma_G |t^s|^4 V_G I_0^s, \tag{1a}$$

$$I_G^p \propto \sigma_G |t^p|^4 \cos^2\theta_p V_G I_0^p, \tag{1b}$$

respectively, where I_0^s and I_0^p are the laser intensity for s and p polarization, respectively; t^s and t^p are the corresponding Fresnel transmission coefficients; σ_G is the Raman cross section; V_G is the sample volume emitting the Raman radiation of the G mode; and θ_p is the refraction angle inside the sample. The intensities of the D mode in far-field Raman measurement are given by

$$I_D^s \propto \sigma_{D,\parallel} |t^s|^4 V_D I_0^s, \tag{2a}$$

$$I_D^p \propto (\sigma_{D,\parallel} \cos^2 \theta_p + \sigma_{D,\perp} \sin^2 \theta_p)|t^p|^4 V_D I_0^p, \quad (2b)$$

where V_D is the sample volume emitting the Raman radiation of the D mode, and $\sigma_{D,\parallel}$ and $\sigma_{D,\perp}$ are the Raman cross sections of the D mode for $E_\parallel$ and $E_\perp$, respectively. In the case of TERS, the Raman intensity of the D mode for p-polarized light I_D^{p*} can be approximated as the sum of the Raman intensity of the unenhanced region of the sample I_D^p and that of the enhanced region, assuming that the volume of the enhanced region V^* is much smaller than that of the unenhanced region:

$$I_D^{p*} - I_D^p \propto \sigma_{D,\perp} \sin^2 \theta_p M^4 |t^p|^4 V^* I_0^p, \quad (3)$$

where $M = E_{loc}/E_0$ is the electric field enhancement factor. M^4 in Eq. (3) is the total Raman enhancement factor [17] and can be derived from Eq. (3) with the use of Eqs. (1) and (2), namely,

$$M^4 = \frac{I_D^{p*} - I_D^p}{I_D^p} \frac{I_D^p/I_D^s}{I_D^p/I_D^s - I_G^p/I_G^s} \frac{V_D}{V^*}. \quad (4)$$

V_D is determined by the size of the focused light spot (~ 2.5 μm) and the width of the grid lines (80 nm extracted from the AFM image) as shown in Fig. 3. V^* is determined by the lateral resolution of our TERS instrument, which is 25 nm. As the ions are assumed to penetrate into the graphite sample for only a few layers, the electromagnetic enhancement factor is considered to be a constant in this region. According to the experimental data presented in Fig. 2 and that obtained from the far-field measurements, $(I_D^{p*} - I_D^p)/I_D^p \approx 3$ and $(I_D^p/I_D^s)/(I_D^p/I_D^s - I_G^p/I_G^s) \approx 10$. With the use of these numbers, the extracted M is ~ 10. Note that the electromagnetic enhancement factor for a covered tip can be found in an independent experiment by the method proposed recently [17].

This work is supported by National Science Council (NSCT) (No. 96-2120-M-002-002) and Academia Sinica in Taiwan.

References

1. K. S. Novoselov, D. Jiang, F. Schedin, T. J. Booth, V. V. Khotkevich, S. V. Morozov, and A. K. Geim, Proc. Natl. Acad. Sci. USA **102**, 10451 (2005).
2. K. S. Novoselov, A. K. Geim, S. V. Morozov, D. Jiang, M. I. Katsnelson, I. V. Grigorieva, S. V. Dubonos, and A. A. Firsov, Nature **438**, 197 (2005).
3. H. B. Heersche, P. Jarillo-Herrero, J. B. Oostinga, L. M. K. Vandersypen, and A. F. Morpurgo, Nature **446**, 56 (2007).
4. F. Tuinstra and J. L. Koenig, J. Chem. Phys. **53**, 1126 (1970).
5. L. G. Cancado, M. A. Pimenta, B. R. A. Neves, M. S. S. Dantas, and A. Jorio, Phys. Rev. Lett. **93**, 247401 (2004).
6. K. Nakamura and M. Kitajima, Phys. Rev. B **45**, 78 (1992).
7. A. C. Ferrari and J. Robertson, Phys. Rev. B **61**, 14095 (2000).
8. A. Hartschuh, E. J. Sanchez, X. S. Xie, and L. Novotny, Phys. Rev. Lett. **90**, 095503 (2003).
9. T. Ichimura, N. Hayazawa, M. Hashimoto, Y. Inouye and S. Kawata, Phys. Rev. Lett. **92**, 220801 (2004).
10. N. Anderson, A. Hartschuh, S. Cronin, and L. Novotny, J. Am. Chem. Soc. **127**, 2533 (2005).
11. B. Pettinger, B. Ren, G. Picardi, R. Schuster, and G. Ertl, Phys. Rev. Lett. **92**, 096101 (2004).
12. C. Thomsen and S. Reich, Phys. Rev. Lett. **85**, 5214 (2000).
13. L. Novotny, E. J. Sanchez, and X. S. Xie, Ultramicroscopy **71**, 21 (1998).
14. D. L. Greenaway, G. Harbeke, F. Bassani, and E. Tosatti, Phys. Rev. **178**, 1340 (1969).
15. A. Gruneis, R. Saito, Ge. G. Samsonidze, T. Kimura, M. A. Pimenta, A. Jorio, A. G. Souza Filho, G. Dresselhaus, and M. S. Dresselhaus, Phys. Rev. B **67**, 165402 (2003).
16. O. Tonomura, Y. Mera, A. Hida, Y. Nakamura, T. Meguro, and K. Maeda, Appl. Phys. A **74**, 311 (2002).
17. M. M. Dvoynenko and J.-K. Wang, Opt. Lett. **32**, 3552 (2007).